

---

# Learning Runtime Decisions for Adaptive Real-Time Perception

---

**Anurag Ghosh<sup>1\*</sup> Akshay Nambi<sup>2</sup> Vaibhav Balloli<sup>2</sup> Aditya Singh<sup>2</sup> Tanuja Ganu<sup>2</sup>**

<sup>1</sup>Carnegie Mellon University <sup>2</sup>Microsoft Research India

anuraggh@cs.cmu.edu, {akshay, t-vballoli, t-adsingh, taganu}@microsoft.com

## Abstract

Real-time perception requires planned resource utilization. Computational planning in real-time perception is governed by two considerations – accuracy and latency. There exist run-time decisions (e.g. choice of input resolution) that induce tradeoffs affecting performance on a given hardware, arising from intrinsic (content, e.g. scene clutter) and extrinsic (system, e.g. resource contention) characteristics.

Earlier runtime execution frameworks employed rule-based decision algorithms and operated with a fixed algorithm latency budget to balance these concerns, which is sub-optimal and inflexible. We propose Chanakya, a learned approximate execution framework that naturally derives from the streaming perception paradigm, to automatically learn decisions induced by these tradeoffs instead. Chanakya is trained via novel rewards balancing accuracy and latency implicitly, without approximating either objectives. Chanakya simultaneously considers intrinsic and extrinsic context, and predicts decisions in a flexible manner. Chanakya, designed with low overhead in mind, outperforms state-of-the-art static and dynamic execution policies on public datasets on both server GPUs and edge devices.

## 1 Introduction

Real-time perception is an important precursor for developing intelligent embodied systems. These systems operate on sensory data on top of a hardware substrate, *viz*, a mix of resource-constrained, embedded and networked computers. Resource planning is a critical consideration in such constrained scenarios. Further, these systems need to be carefully designed to be latency sensitive and ensure safe behaviour (See Figure 1).

Many runtime execution decisions exist, e.g. the spatial resolution (scale) to operate at, temporal stride of model execution, choice of model architecture etc. The runtime decisions are influenced by (a) intrinsic context derived from sensor data (e.g. image content) (b) extrinsic context observed from system characteristics, e.g. contention from external processes (other applications). A execution framework is needed to use available context, jointly optimize accuracy and latency while taking these decisions.

Traditional execution frameworks [1, 2, 3, 4] operate in the following paradigm – optimize model to operate within a latency budget. Largely, they do not jointly optimize accuracy and latency for real-time tasks. Instead, they optimize proxies like latency budget [1], input resolution [2], latency from resource contention [4] or energy [5]. Their approach requires rule-based decision making – heuristic design for every characteristic, instead of learning the decision function. These frameworks explicitly handcraft rules to accommodate hardware capabilities. Moreover, traditional strategies (Figure 1) budgeting latency are suboptimal when operating on streaming data [6].

---

\*Work done at Microsoft Research India

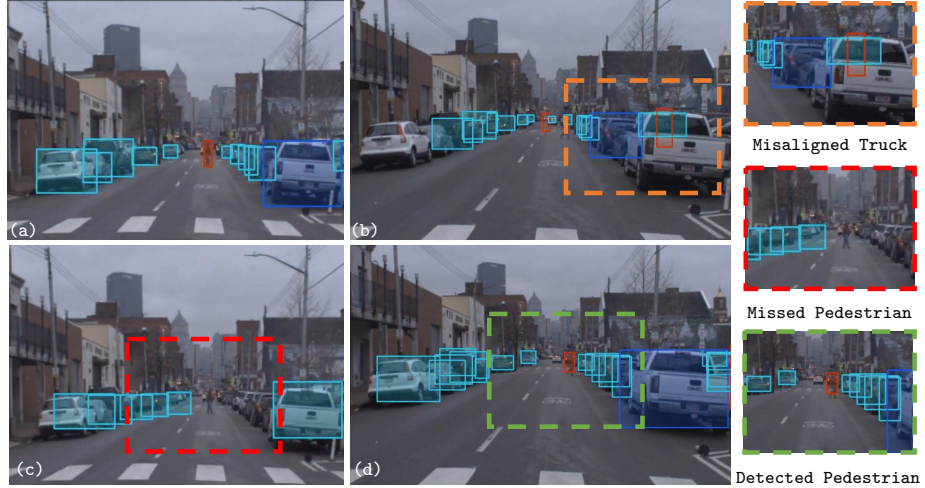


Figure 1: **Optimizing real-time perception inference.** (a) A powerful detector (HTC [7]) has very good offline (non real-time) ( $38.2\text{ mAP}$ ) performance. (b) However, by the time it finishes execution ( $750ms$  per frame), inferences are not aligned with objects ( $6.2\text{ sAP}$ ). (c) Solely optimizing for latency via a faster model ( $30ms$ , RetinaNet [8] at low resolution) leads to suboptimal and unsafe behavior ( $6.0\text{ sAP}$ ), like missing pedestrians. (d) Learning decisions with favourable inference tradeoffs with Chanakya ( $21.3\text{ sAP}$ ) achieves better real-time performance.

Operating in the new streaming perception paradigm, we propose Chanakya<sup>2</sup> – a novel learning-based approximate execution framework to learn runtime decisions for real-time perception. Chanakya operates in the following manner – (a) Content and system characteristics are captured by intrinsic and extrinsic context which guide runtime decisions. (b) Decision classes are defined, such as the input resolution (scale) choices, the model choices etc. Chanakya handles these interacting decisions and their tradeoffs which combinatorially increase. (c) Accuracy and latency are jointly optimized using a novel reward function without approximating either objectives. (d) Execution policy is learnt from streaming data, and is dynamic, i.e. configuration changes during real-time execution of the perception system.

Chanakya learns performant execution policies and can incorporate new decision dimensions, stochastic system context and be ported to different hardware. Importantly, our improvements are in addition to, and complementary to models and the decision dimensions themselves – faster & more accurate models [9, 10], vision-guided runtime decisions [11, 12, 13] and system-focused decisions [14, 15] can be easily incorporated.

## 2 Related Work

**Flexible Real-Time Decision Making.** Intelligent systems that are reactive [16] and flexible [17] are well studied. Our work is related to classical resource utilization and scheduling literature [18] and theoretical frameworks for real-time reinforcement learning in asynchronous environments [19, 20].

Contrasting with prior RL based execution frameworks [3, 21] which are operating in the suboptimal traditional latency budget paradigm [6], Chanakya is situated in the streaming perception paradigm. The key challenge for all these works has been the difficulty in designing rewards to jointly optimize accuracy and latency, and previous frameworks have learnability issues (See Section 3.4). We propose Chanakya with a novel reward and asynchronous training procedure for training approximate execution frameworks on large public datasets.

**Real-time Perception and Video Analytics.** In the vision community, accuracy-latency pareto decisions or “sweet spots” for vision models have been studied [22, 6]. Drawing from these inferences, proposed design decisions exploit spatial [11, 13] and temporal [10] redundancies and improve real-time perception. These works are complementary to our work, and their meta-parameters can be

<sup>2</sup>Chanakya was an ancient Indian polymath, known for good governance strategies balancing economic development and social justice.

learned via Chanakya, and changed at runtime (static in their work). Improved backbones [23, 24, 9], compression techniques like quantization [25] and pruning [26] are also complementary.

In the systems community, Chanakya is related to video analytics efforts for the edge and cloud, wherein works aim to optimize design decisions [15, 27, 14, 28, 29] during training and inference. Chanakya can incorporate their decision designs during inference (like AdaScale [2]). For example, LegoDNN [15] decides which NN blocks to use via a novel optimization formulation, which instead can be learned via Chanakya. Mistify and Ekyा [14, 29] tailor models considering offline accuracy, latency and concept drift and these model choices can be selected by Chanakya at runtime.

**Approximate Execution Frameworks.** Many approximate execution frameworks have been designed for real-time perception. However, instead of maximizing real-time performance, they optimize proxies such as energy [5], latency from contention [4], or latency budget [1] and employ handcrafted rule-based heuristics. Previous works [4] have also highlighted the need for reinforcement learning (RL) based methods to learn runtime decisions. Chanakya instead learns runtime decisions to maximize streaming performance conditioned on intrinsic and extrinsic context, operating on a variety of decision dimensions.

Many systems frameworks describe runtime decisions such as changing input resolution [2, 30], switching between models [1, 30], changing model configurations with latency [4], selecting frames to execute models vs trackers [31, 5], deciding between remote execution on the cloud and local execution on the edge [31, 32, 33]. These decisions can be learnt by Chanakya.

### 3 Chanakya: Learned Execution Framework for Real-Time Perception

#### 3.1 Background on Streaming Perception

Traditionally, for real-time perception, model is executed at input video’s frequency, say, 30 FPS. Thus the model is constrained to process a frame within a latency budget, in this case, 33 ms per frame. Streaming perception [6] instead places a constraint on the algorithm’s output, no constraints are placed on the underlying algorithm. The constraint is – *anytime the algorithm is queried, it must report the current world state estimate at that time instant*.

**Formal Definition:** Input stream comprises of sensor observation  $x$ , ground truth world state  $y$  (if available) and timestamp  $t$ , denoted by  $\{O_i : (x_i, y_i, t_i)\}_{i=1}^T$ . Till time  $t$ , algorithm  $f$  is provided  $\{(x_i, t_i) | t_i < t\}$ . Algorithm  $f$  generates predictions  $\{(f(x_j), s_j)\}_{j=1}^N$ , where  $s_j$  is the timestamp when a particular prediction  $f(x_j)$  is produced. This output stream is *not* synchronised with input stream and is not necessarily operating on every input. Real-time constraint is enforced by comparing the most recent output  $f(x_{\varphi(t)})$  to ground truth  $y_i$ , where  $\varphi(t) = \text{argmax}_j s_j \leq t$ .

**Throughput vs Latency.** Assuming two hardware setups, one with a single GPU available and another with infinite GPU’s available (simulated), we employ a Faster R-CNN detector (no forecaster) on a P40 GPU. The sAP scores obtained are 13.9 sAP and 15.7 sAP respectively. Additional compute (GPU’s) improves system throughput, but does not improve latency of real-time execution. Thus it is not a solution for improving real-time perception.

#### 3.2 High Level Overview

We design a learned execution framework for real-time perception that jointly optimizes accuracy and latency. We consider object detection to be the instantiation of our perception problem, however, the described principles apply without loss of generality.

Consider real-time object detection. The real-timeliness requirement of streaming perception is fulfilled by pairing our detector (say Faster R-CNN) with object tracker (Tracktor [34]) and state estimator (Kalman Filter). We can change meta-parameters like detector’s and tracker’s scale, temporal stride of tracker along with internal parameters (for instance, number of proposals in the detector) and generalize this to include the choice of components themselves (the detector/tracker etc). Consider these decisions to be configuration of the algorithm  $f$ , and a policy  $\pi$  that emits this configuration. We wish to learn a controller that governs the execution policy  $\pi^*$ , which is triggered periodically to decide the runtime configuration. In this work, we assume that all the other components (detector, tracker etc) have been trained already and we solely learn the controller.

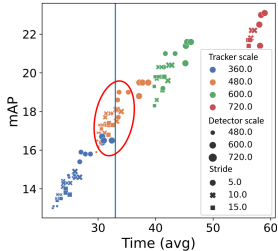


Figure 2: **Configuration trade-offs of a perception system.** Many configurations (tracker scale, detector scale, temporal stride, number of proposals). Configs. in red ellipse satisfy real-time budget 33ms.

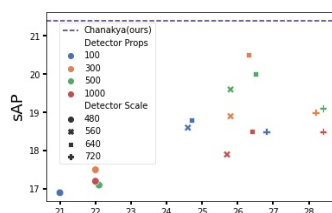


Figure 3: **Offline vs Real-time Perception.** mAP vs sAP for different configurations of same system. An increase in offline performance (mAP) doesn’t imply an increase in real-time performance (sAP).

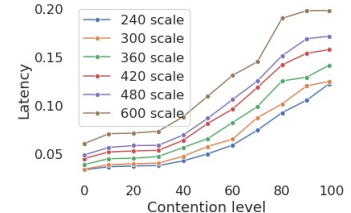


Figure 4: **Extrinsic Factors.** Process contention is dynamic, and induces latency differences for a detector (Faster-RCNN) at a given scale. Notice that this relationship is non-linear. Other components follow similar trends.

We formulate learning the runtime decision as a deep contextual bandit problem, where a sequence of independent trials are conducted and in every trial the controller chooses a configuration (i.e. action)  $a$  from the set of possible decisions  $\mathbb{D}$  along with the provided context  $z$ . After a trial the controller receives a reward  $r$  as feedback for the chosen configuration and updates the execution policy. As we will see in Section 3.3, intrinsic and extrinsic factors affect policy  $\pi$ . Thus we define context  $z$  encapsulating these factors which is provided to the controller. We learn a  $Q$ -function  $Q_\theta(z, a)$ , for every action  $a$  given context  $z$ , where  $Q$ -values define the policy  $\pi$  to configure  $f$ .

### 3.3 Intrinsic and Extrinsic Context Guide Runtime Decisions

Numerous factors inform runtime decisions in real-time perception. Figure 2 depicts configurations for a predefined perception system. Randomly picking a “good” configuration (marked by red ellipse) can result in a sub-optimal decision, causing a drop of at least 3 mAP in comparison to the “optimal” configuration. Optimal decision shifts with hardware change, on Argoverse-HD using a P40 GPU, the best scale turns out to be 600 instead of 900 on a 1080Ti GPU [6]. Selection of algorithm components (say, the detector) is itself a decision with trade-offs [22]. Detection models exhibit different kinds of errors [35, 36], and changing the scale affects their performance. Lastly, offline and real-time perception performance are not correlated (Figure 3).

Intrinsic factors like image content influence decisions – static configurations are sub-optimal. E.g., We can optimize scale at runtime [2] based on video content to improve throughput while maintaining accuracy. Extrinsic factors introduce additional challenges. Optimal decisions change with the stochastic nature of the external process, such as resource contention induced by other running processes. Figure 4 shows change in latency with contention levels and this relationship is non-linear. Other such extrinsic factors include network conditions and power considerations. Extrinsic context are non-differentiable, thus we do not use an end-to-end network to learn the overall context  $z$ .

We concatenate outputs of the following functions to form the overall context to the controller,

- 1. Switchability Classifier:** Models exhibit different error characteristics, motivating the need to switch models at runtime [1]. Switchability classifier guides model switching at runtime.
- 2. Adaptive Scale Regressor:** AdaScale [2] predicts the optimum scale an image should be inferred at, such that *single frame latency* is minimized. We use their regressor as an intrinsic context.
- 3. Contention Sensor:** Process Contention affects model latency. We employ the GPU contention generator and sensor from [4], simulating discrete contention levels.
- 4. Scene aggregates:** We also compute frame-level aggregates: (i) **Confidence Aggregates:** We compute the mean and the standard deviation of the confidence value associated with the predictions. The intuition is if the average confidence is low, which might indicate execution of an “expensive” configuration. (ii) **Category Aggregates:** We count of instances of each category in the predictions. This might capture *rare* objects, which may require additional resources to be localized. (iii) **Object Size Aggregates:** We categorize and aggregate predictions as small, medium and large detections (like COCO thresholds [37]). This is useful as small objects are considered difficult to detect.

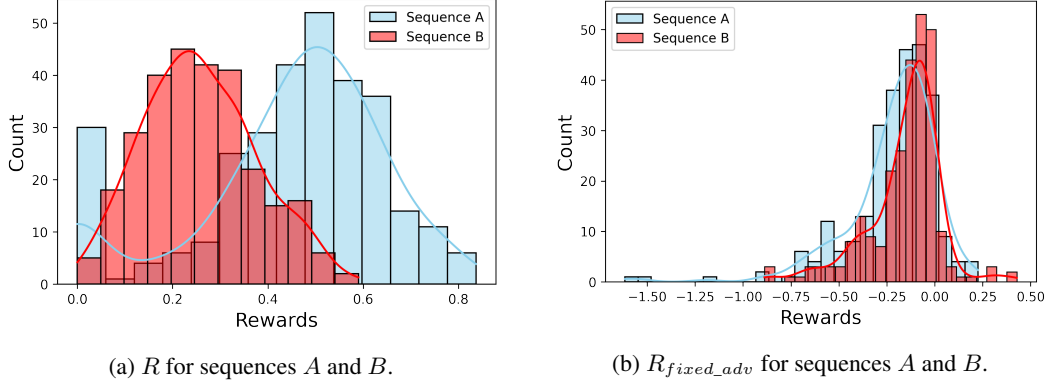


Figure 5: **Understanding  $R_{fixed\_adv}$ .** In many video sequences, performance measure (single frame loss  $L$ ) is high for all configurations (e.g. all objects are large, highly visible), such as Sequence A. Compared to sequences (like B) where performance is lower and more heavily dependent on detector type and scale (e.g. objects are small or occluded).  $R_{fixed\_adv}$  corrects this bias.

### 3.4 Reward Jointly Optimizes Latency And Accuracy

Traditionally, output  $\hat{y}_i$  is emitted for observation  $O_i$  at time  $\hat{t}_i$  ( $> t_i$ ), and the reward [3, 21] is defined as

$$R_{trad} = \phi(y_i, \hat{y}_i) + \lambda \xi(t_i, \hat{t}_i)$$

considering accuracy via  $\phi$  and latency via  $\xi$  separately. However, hyperparameter  $\lambda$  for this additive reward is globally inconsistent (i.e. changes depending on intrinsic/extrinsic context) which doesn't work for large datasets. In our experiments we observed that controller collapsed to predict a single configuration when rewards of this form were provided (depending on  $\lambda$ ), and did not learn.

Our rewards optimize accuracy and latency simultaneously. Intuitively, reward  $R$  compares the model output with a ground truth stream of the actual world state. Assume algorithm  $f$  is governed by policy  $\pi$  receives observation  $O_x$ , controller performs action  $a_x$  at time  $t_x$  to configure  $f$  and another observation  $O_y$  with action  $a_y$  is taken at  $t_y$  ( $t_y > t_x$ ). We propose a reward,

$$R(t_x, t_y) = L(\{y_{t_k}, \hat{y}_{\varphi(t_k)}\}_{k=x}^y) \quad (1)$$

where  $L$  is an arbitrary single frame loss. Intuitively, the reward for action  $a_x$  is streaming accuracy obtained for a stream sequence segment until a new action  $a_y$  is taken in the future and  $\varphi$  (defined in Section 3.1) ensures only real-time results are accounted for. Reward  $R(t_x, t_y)$  ensures learned controller implicitly considers real-time constraints and accuracy of the decision  $a_x$ , not assuming any properties of the algorithm  $f$  or loss  $L$ . Thus, it can be applied to other perception tasks.

While [6] defined  $L_{streaming} = L(\{y_{t_k}, \hat{y}_{\varphi(t_k)}\}_{k=0}^N)$  and corresponds to  $R(0, T)$  (Loss over  $N$  observations from a video stream of length  $T$ ),  $L_{streaming}$  was employed to characterize performance of  $f$  on the sensor stream. Directly employing it as reward made training the controller sample-inefficient, and did not converge before we exhausted our training budget.

While reward proposed in Equation 1 is learnable, it is biased towards the inherent characteristics of the video sequence. Consider two video sequences  $A$  and  $B$ , Sequence  $A$  with one large object that can be easily detected would have much higher average rewards than Sequence  $B$  with many occluding and small objects. To normalize for this factor, we consider a fixed policy  $\pi_{fixed}$ , i.e., a fixed configuration of algorithm  $f$  and propose,

$$R_{fixed\_adv}(t_x, t_y) = R_\pi(t_x, t_y) - R_{\pi_{fixed}}(t_x, t_y) \quad (2)$$

where  $R_{\pi_{fixed}}$  is the reward obtained by executing algorithm  $f$  following a fixed policy. To implement  $R_{fixed\_adv}$ ,  $f$  with fixed policy  $\pi_{fixed}$  are executed and prefetched the predictions and the timestamps are stored. During training, we compute  $R_\pi$  and load  $\pi_{fixed}$  outputs to simulate  $R_{\pi_{fixed}}$ .

This eliminates the bias in the initial proposed reward, and provides the *advantage* of learned policy over fixed policy (See Figure 5). In Section 4.1, we show any fixed policy configuration ( $\pi_{fixed}$ ) suffices and the policy learned is resilient to variations of this selection. We refer to the reward in Equation 1 as  $R_1$  and Equation 2 as  $R_2$  in our experiments for simplicity.

Table 1: **Improvements on a predefined system.** Chanakya outperforms competing execution policies for a predefined system. All the execution policies operate on top of a perception system employing the same components: Faster R-CNN and Kalman Filter.

Approach	<i>sAP</i>	<i>sAP<sub>50</sub></i>	<i>sAP<sub>75</sub></i>
1. Streamer (s=900) [6] (Static Policy)	18.2	35.3	16.8
2. Streamer (s=600) [6] (Static Policy)	20.4	35.6	20.8
3. Streamer (s=600, np=300) (Static-Expert Policy)	20.8	36.0	20.9
4. Streamer (s=600, np=500) (Static-Expert Policy)	20.9	35.9	20.9
5. Streamer + AdaScale [2] (Dynamic-Traditional Policy)	13.4	23.1	13.8
6. Streamer + AdaScale + Our Scheduler (Dynamic-Trad. Policy)	13.8	23.4	14.3
<b>7. Chanakya (s<sub>1</sub>, np<sub>1</sub>, R=R<sub>1</sub>)</b>	21.0	36.8	<b>21.2</b>
<b>8. Chanakya (s<sub>1</sub>, np<sub>1</sub>, R=R<sub>2</sub>, π<sub>fixed</sub>=(s=480, np=300))</b>	<b>21.3</b>	<b>37.3</b>	21.1
9. Offline Upper Bound (s=600, Latency Ignored)	24.3	38.9	26.1

### 3.5 Controller Design Decisions

Due to severe real-time constraints, we considered individual frames as independent trials while learning our controller (E.g., we compute context from a single frame) to incur minimal overhead (amortized overhead of around 1%). Considering sequences as controller’s input incurred significant overheads and impeded performance. While Chanakya employs deep contextual bandits, other algorithms are applicable.

**Combinatorially Increasing Configurations.** Consider decision space  $\mathbb{D} = \{D_1, D_2..D_m\}$ , with dimensionality  $M = |\mathbb{D}|$ , where each decision dimension  $D_i$  corresponds to a configuration parameter of the algorithm  $f$  discretized as  $d_k$ . Thus, an action  $a$  has  $M$  decision dimensions and each discrete *sub-action* has a fixed number of choices. For example, if we consider 2 decision dimensions,  $\mathbb{D} = \{D_{scale}, D_{model}\}$ , the potential configurations would be  $D_{scale} = \{720, 600, 480, 360, 240\}$ ,  $D_{model} = \{yolo, fcos, frcnn\}$ . Using conventional discrete-action algorithms,  $\prod_{d \in \mathbb{D}} |d|$  possible actions need to be considered. Efficiently exploring such large action spaces is difficult, rendering naive discrete-action algorithms like [3, 21] intractable.

Chanakya uses a multi-layer perceptron for predicting  $Q_\theta(z, a_i)$  for each sub-action  $a_i$  and given context  $z$ , and employs action branching architecture [38] to separately predict each sub-action, while operating on a shared intermediate representation. This significantly reduces the number of action-values to be predicted from  $\prod_{d \in \mathbb{D}} |d|$  to  $\sum_{d \in \mathbb{D}} |d|$ .

**Real-time Scheduler.** Choosing which frames to process is critical to achieve good streaming performance. Temporal aliasing, i.e., the mismatch between the output and the input streams, reduces performance. [6] prove optimality of shrinking tail scheduler. However, this scheduler relies on the assumption that the runtime  $\rho$  of the algorithm  $f$  is constant. This is reasonable as runtime distributions are unimodal, without considering resource contention.

Chanakya changes configurations at runtime, and corresponding  $\rho$  changes. Fortunately, our space of configurations is *discrete*, and  $\rho$ ’s (for *every* configuration) can be assumed to be constant. Thus, a fragment of the sequence where a particular configuration is selected is a scenario where shrinking tail scheduler using that runtime will hold. We cache configuration runtimes of algorithm  $f$  and *modify the shrinking tail scheduler* to incorporate this assumption.

**Asynchronous Training.** Chanakya is trained in such a way that real-time stream processing is simulated, akin to challenges presented in [19, 20]. Thus, a key practical challenge is to factor in average latency for generating the context from the observations, computing the controller’s action during training. We also need to ignore the time taken to train the controller as these would disrupt and change the system performance. Training the controller concurrently on a different GPU incurred high communication latency overhead.

**Training for edge devices.** We emulate training the controller for edge devices on a server by using the measured runtimes for each configuration on the edge device, since Chanakya only requires the runtimes of the algorithm  $f_\pi$  on the target device to train the controller.

Table 2: **Handling large decision spaces.** We incorporate a tracker in our predefined perception system. Choice of detector scale and proposals, tracker scale and stride, combinatorially expands our decision space. Chanakya is able to learn a competitive policy compared to best static policies [6].

Approach	sAP
Static Policy (s=900, ts=600, k=5)	17.8
Static Policy (s=600, ts=600, k=5)	19.0
Chanakya ( $s_1, np_1, ts, k, R_2$ )	<b>19.4</b>

Table 3: **Learning decisions from scratch.** Chanakya is able to decide model and other meta-parameter choices even when optimal algorithmic components are unknown.

Approach	sAP
Static Policy (m= $f_{cos}$ , s=600)	16.7
Static Policy (m= $yolov3$ , s=600)	20.2
Static Policy (m= $frcnn$ , s=600)	20.4
Chanakya (m= $m$ , $s_1, np_1, R=R_2$ )	<b>20.7</b>

## 4 Experiments and Results

We analyse and evaluate Chanakya through the following experiments. We employ sAP metric [6] that coherently evaluates real-time perception, combining latency and accuracy into a single metric. It is non-trivial to compare traditional systems that use mAP and latency for evaluation as their algorithms would require major modifications. However, we do augment one such method, AdaScale [2] by incorporating Kalman Filter and our scheduler. Apart from this, we compare our approach with static policies obtained from benchmarking. Please note Chanakya’s improvements are complementary and in addition to the system components themselves, newer models would lead to further improvements. All the results are reported on Argoverse-HD, additional results on Imagenet-VID can be viewed in Appendix A, along with implementation details.

**Improvements on a predefined system.** For a real-time perception system on a given hardware (P40 GPU), let’s assume system components – detector (Faster R-CNN), scheduler (Modified Shrinking Tail) and forecaster (a Kalman Filter) are known. We optimize configurations across two decision dimensions  $\mathbb{D} = \{D_s : \{360, 480, 540, 640, 720\}, D_{np} : \{100, 300, 500, 1000\}\}$ , i.e., detector scale and number of proposals. We evaluate Chanakya using both variants of rewards described in Section 3.4, and only intrinsics are provided as context. We compare with best performing configurations reported by [6] (**static policy**). Further, we asked an expert who employed domain knowledge [22] to optimize the proposal decision dimension via benchmarking (**static expert policy**). We also compare with a **dynamic traditional policy**, AdaScale [2] which predicts input scale and is trained to minimize single frame latency as it is situated in traditional latency budget paradigm. Table 1 shows that we outperform all of these methods, as Chanakya can adapt dynamically (See Figure 6) via context which explains improvement over static policies and considers the real-time constraint holistically. Chanakya does not *solely* minimize single frame latency which explains improvements over the traditional policy. Similar trends hold for ImageNet-VID, please see Supplementary.

**Learning decisions from scratch.** Consider when optimal components (say, the detection model or tracker) are unknown for a given hardware. We will now introduce the third dimension, which is the choice of the model (FCOS or YOLOv3 or Faster R-CNN). Chanakya has to pick configurations across model choices, scale choices and proposal choices (if applicable, decision dimension is ignored otherwise). Using an alternative detector, i.e, FCOS and with the best scale obtained via benchmarking (paired with Streamer [6]), the static policy has an sAP of 16.7, while Chanakya has sAP of 20.7 (23% improvement). Similar performance improvement (+5.5 sAP) was also seen on ImageNet-VID.

**Handling large decision spaces.** We extend our pre-defined system (Faster R-CNN + Scheduler + Kalman Filter) with a tracker (Tracktor [34]). Tracker supports configuration of tracker scale and temporal stride, i.e. number of times it’s executed versus the detector, apart from detector scale, number of proposals, increases the decision space to 500 configurations. It is not feasible to explore the entire decision space using brute-force if we consider deployment to many hardware platforms. In contrast, our approach learned the execution policy in 5 training epochs. As shown in Table 2, Chanakya learns a competitive policy that outperforms the **best static policy** from [6] by +1.6 sAP.

**Performance and configuration shift on edge devices.** We consider deploying the predefined system discussed earlier on two edge devices – Jetson Xavier NX and Xavier AGX. We employ emulated

Scales		Proposals			
		100	300	500	1000
360	360	0.00	0.00	0.02	0.00
	480	0.09	0.14	0.41	0.00
	560	0.01	0.17	0.16	0.01
	640	0.00	0.00	0.00	0.00
	720	0.00	0.00	0.00	0.00

Figure 6: **Dynamic Configurations executed on P40 GPU.** For the predefined system, Chanakya changes the configuration depending on the intrinsics and achieves better performance.

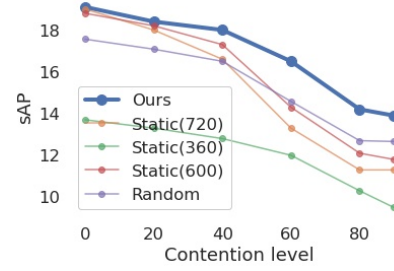


Figure 7: **Chanakya adapts to extrinsic factors.** Compared to static execution policies, Chanakya has better performance at different levels of GPU contention and degrades less at higher contention.

Scales		Proposals			
		100	300	500	1000
360	360	0.00	0.00	0.06	0.00
	480	0.00	0.00	0.00	0.00
	560	0.00	0.00	0.04	0.00
	640	0.00	0.03	0.55	0.06
	720	0.03	0.01	0.18	0.03

(a) Xavier NX

Scales		Proposals			
		100	300	500	1000
360	360	0.00	0.00	0.02	0.01
	480	0.00	0.01	0.05	0.00
	560	0.00	0.01	0.00	0.00
	640	0.01	0.03	0.78	0.05
	720	0.00	0.00	0.03	0.00

(b) Xavier AGX

Figure 8: **Configuration shift on edge devices.** The predefined system is deployed on the edge devices. Chanakya is trained via emulation, and we observe a shift in chosen configurations that matches our expectations for these hardware platforms.

training procedure discussed in Section 3.5. From Table 4 comparing performance on Xavier NX, Chanakya improves sAP by 12% and 28% Argoverse-HD and ImageNet-VID respectively over static policies found by benchmarking. In Figure 8, we observe shifts in configurations selected for the two devices (compared to Figure 6 evaluated on a server GPU P40). Xavier AGX is more powerful, and we observe more frequent selection of higher detection scale ( $s = 480$ ) compared to Xavier NX, in line with our expectations.

**Adapting to Extrinsic Factors.** In our predefined system, we consider contention as our extrinsic factor and study Chanakya’s behaviour, assuming black-box resource contention levels available at run-time. This scenario is common on smartphones/edge devices [4] where multiple processes employ the same resource. Static policies, wherein decisions are not made considering contention would degrade quickly (See Section 3.3).

Chanakya adapts to sensed contention level (provided as context) by choosing decisions which correspond to the sweet-spot for that contention level, with no additional modifications. Critically, Chanakya is flexible and adapts decisions to the contention level unlike [4] who explicitly model the problem as a rule-based system (modeling latency and accuracy with quadratic regression models) and handcraft a contention-aware scheduler. Performance degrades across all approaches with increasing contention and Figure 7 Chanakya is able to adapt better than static policies.

**New hardware and action spaces.** Consider the task of migrating a streaming perception system from a device employing P40 GPU, to newer V100 GPU. New hardware has additional features, such as faster inference at lower precision levels (P40 in comparison does offer limited support; few FP16 operations are faster). As the tradeoffs have shifted, we do not assume that components and hardware optimizations are known. We consider additional decisions – choice between inference at FP32 and FP16 and choice between models. We employed Chanakya with the following decision space:  $\mathbb{D} = \{D_m : \{resnet\_frn, swin\_frn, resnet\_cascade\_rcn, swin\_cascade\_rcn\}, D_p : \$

Table 4: **Performance on edge devices.** Comparisons on Xavier-NX edge device. We can observe that Chanakya improves performance over static policies on both the datasets. Also note that the controller was trained on the server, and deployed on the constrained edge device.

Approach	Argoverse-HD (sAP)	ImageNet-VID (sAP)
Streamer (s=560, np=500) (Static Policy) [6]	7.8	18.8
Streamer (s=640, np=300) (Static Policy) [6]	7.4	20.0
Streamer with Random Selection	7.6	17.5
Chanakya ( $R = R_1$ )	8.1	19.4
Chanakya ( $R = R_2$ )	<b>8.3</b>	<b>22.4</b>

Table 5: **Importance of Context.** All components of the considered context contribute to improved real-time performance.

Dropped feature	sAP
None	<b>21.3</b>
Adaptive Scale	19.2
Category aggregates	19.4
Confidence aggregates	20.3
Object size aggregates	20.4

Table 6: **Resilience.** Chanakya learns performant decisions despite using a bad fixed policy. Changing Chanakya’s action space from  $s_1$  to  $s_2$  also does not affect performance significantly.

Approach	sAP
Ours ( $s_1, np_1, R_2, \pi_{fix} = (640, 300)$ )	<b>21.3</b>
Ours ( $s_1, np_1, R_2, \pi_{fix} = (480, 300)$ )	<b>21.3</b>
Ours ( $s_1, np_1, R_2, \pi_{fix} = (360, 1000)$ )	21.1
Ours ( $s_2, np_1, R_1$ )	18.2
Ours ( $s_2, np_1, R_2$ )	<b>20.4</b>

$\{FP32, FP16\}, D_s : \{800, 880, 960, 1040, 1120, 1200\}, D_{np} : \{100, 300, 500, 1000\}\}$ . Without benchmarking and domain expertise, it’s non-trivial to decide these meta-parameters.

We consider the best known static policy (employing Faster R-CNN with Resnet-50 at  $s = 900$ ) proposed by [6] for V100 GPU as our baseline which has 18.3 sAP. Chanakya obtained 27.0 sAP, i.e., +8.7 sAP (47%) improvement. This is the highest achieved improvement on the Streaming Perception Challenge without using additional data.

#### 4.1 Ablation Studies

We discuss some of the considerations of our approach, we employ Chanakya on our pre-defined perception system.

**Importance of Context.** Table 5 shows that when a context feature is dropped performance reduces by  $\approx 1$  sAP. Context overheads can be viewed in Supplementary.

**Resilience.** Table 6 shows that Chanakya is resilient to the choice of the initial fixed policy  $\pi_{fixed}$  used in our reward function  $R_2$ . Chanakya arrives at a competitive policy even if a bad fixed policy is chosen, (360, 1000), which employs very small scale and the maximum number of proposals. Chanakya is resilient to the choice of action space as changing scale space from  $s_1$  to  $s_2$  yielded competitive performance.

## 5 Conclusion

**Limitations and Broader Impact.** While our method does not directly enable unethical applications, it might be employed to deploy and improve such applications. Further study of regulatory mechanisms for safe ML deployments and the impact of methods like Chanakya is required.

We presented Chanakya, a learned runtime execution framework to optimize runtime decisions for real-time perception systems. Our learned controller is efficient, flexible, performant and resilient in nature. Chanakya appears useful for many real-time perception applications in the cloud and edge. We plan to extend this work to scenarios wherein the downstream applications require hard performance guarantees.

## References

- [1] Seungyeop Han, Haichen Shen, Matthai Philipose, Sharad Agarwal, Alec Wolman, and Arvind Krishnamurthy. Mcdnn: An approximation-based execution framework for deep stream processing under resource constraints. In *MobiSys*, 2016.
- [2] Ting-Wu Chin, Ruizhou Ding, and Diana Marculescu. Adascale: Towards real-time video object detection using adaptive scaling. In *MLSys*, 2019.
- [3] Ning Chen, Siyi Quan, Sheng Zhang, Zhuzhong Qian, Yibo Jin, Jie Wu, Wenzhong Li, and Sanglu Lu. Cuttlefish: Neural configuration adaptation for video analysis in live augmented reality. *Transactions on Parallel and Distributed Systems*, 2020.
- [4] Ran Xu, Chen-lin Zhang, Pengcheng Wang, Jayoung Lee, Subrata Mitra, Somali Chaterji, Yin Li, and Saurabh Bagchi. ApproxDet: content and contention-aware approximate object detection for mobiles. In *Sensys*, 2020.
- [5] Kittipat Apicharttrisorn, Xukan Ran, Jiasi Chen, Srikanth V Krishnamurthy, and Amit K Roy-Chowdhury. Frugal following: Power thrifty object detection and tracking for mobile augmented reality. In *Sensys*, 2019.
- [6] Mengtian Li, Yu-Xiong Wang, and Deva Ramanan. Towards streaming perception. In *ECCV*, 2020.
- [7] Kai Chen, Jiangmiao Pang, Jiaqi Wang, Yu Xiong, Xiaoxiao Li, Shuyang Sun, Wansen Feng, Ziwei Liu, Jianping Shi, Wanli Ouyang, et al. Hybrid task cascade for instance segmentation. In *CVPR*, 2019.
- [8] Tsung-Yi Lin, Priya Goyal, Ross Girshick, Kaiming He, and Piotr Dollár. Focal loss for dense object detection. In *ICCV*, 2017.
- [9] Ze Liu, Yutong Lin, Yue Cao, Han Hu, Yixuan Wei, Zheng Zhang, Stephen Lin, and Baining Guo. Swin transformer: Hierarchical vision transformer using shifted windows. In *ICCV*, 2021.
- [10] Jinrong Yang, Songtao Liu, Zeming Li, Xiaoping Li, and Jian Sun. Real-time object detection for streaming perception. In *CVPR*, 2022.
- [11] Chittesh Thavamani, Mengtian Li, Nicolas Cebron, and Deva Ramanan. Fovea: Foveated image magnification for autonomous navigation. In *ICCV*, 2021.
- [12] Babak Ehteshami Bejnordi, Amirhossein Habibian, Fatih Porikli, and Amir Ghodrati. Salisa: Saliency-based input sampling for efficient video object detection. In *ECCV*, 2022.
- [13] Anurag Ghosh, N Dinesh Reddy, Christoph Mertz, and Srinivasa G Narasimhan. Learned two-plane perspective prior based image resampling for efficient object detection. In *CVPR*, 2023.
- [14] Peizhen Guo, Bo Hu, and Wenjun Hu. Mistify: Automating DNN model porting for On-Device inference at the edge. In *NSDI*, 2021.
- [15] Rui Han, Qinglong Zhang, Chi Harold Liu, Guoren Wang, Jian Tang, and Lydia Y Chen. Legodnn: block-grained scaling of deep neural networks for mobile vision. In *MobiCom*, 2021.
- [16] Michael P Georgeff and Amy L Lansky. Reactive reasoning and planning. In *AAAI*, 1987.
- [17] Eric J Horvitz. *Computation and action under bounded resources*. PhD thesis, 1990.
- [18] Mark Boddy and Thomas L Dean. Deliberation scheduling for problem solving in time-constrained environments. *Artificial Intelligence*, 1994.
- [19] Simon Ramstedt and Chris Pal. Real-time reinforcement learning. *NeurIPS*, 2019.
- [20] Jaden B Travnik, Kory W Mathewson, Richard S Sutton, and Patrick M Pilarski. Reactive reinforcement learning in asynchronous environments. *Frontiers in Robotics and AI*, 2018.
- [21] Young Geun Kim and Carole-Jean Wu. Autoscale: Energy efficiency optimization for stochastic edge inference using reinforcement learning. In *MICRO*, 2020.
- [22] Jonathan Huang, Vivek Rathod, Chen Sun, Menglong Zhu, Anoop Korattikara, Alireza Fathi, Ian Fischer, Zbigniew Wojna, Yang Song, Sergio Guadarrama, et al. Speed/accuracy trade-offs for modern convolutional object detectors. In *CVPR*, 2017.

- [23] Andrew Howard, Mark Sandler, Grace Chu, Liang-Chieh Chen, Bo Chen, Mingxing Tan, Weijun Wang, Yukun Zhu, Ruoming Pang, Vijay Vasudevan, et al. Searching for mobilenetv3. In *ICCV*, 2019.
- [24] Xiangyu Zhang, Xinyu Zhou, Mengxiao Lin, and Jian Sun. Shufflenet: An extremely efficient convolutional neural network for mobile devices. In *CVPR*, 2018.
- [25] Song Han, Huizi Mao, and William J Dally. Deep compression: Compressing deep neural networks with pruning, trained quantization and huffman coding. *arXiv preprint arXiv:1510.00149*, 2015.
- [26] Ji Lin, Yongming Rao, Jiwen Lu, and Jie Zhou. Runtime neural pruning. In *NeurIPS*, 2017.
- [27] Shiqi Jiang, Zhiqi Lin, Yuanchun Li, Yuanchao Shu, and Yunxin Liu. Flexible high-resolution object detection on edge devices with tunable latency. In *MobiCom*, 2021.
- [28] Xu Zhang, Yiyang Ou, Siddhartha Sen, and Junchen Jiang. SENSEI: Aligning video streaming quality with dynamic user sensitivity. In *NSDI*, 2021.
- [29] Romil Bhardwaj, Zhengxu Xia, Ganesh Ananthanarayanan, Yuanchao Shu, Nikolaos Karianakis, Kevin Hsieh, Paramvir Bahl, and Ion Stoica. Ekyu: Continuous learning of video analytics models on edge compute servers. In *NSDI*, 2022.
- [30] Ran Xu, Jinkyu Koo, Rakesh Kumar, Peter Bai, Subrata Mitra, Ganga Meghanath, and Saurabh Bagchi. Approxnet: Content and contention aware video analytics system for the edge. *arXiv preprint arXiv:1909.02068*, 2019.
- [31] Tiffany Yu-Han Chen, Lenin Ravindranath, Shuo Deng, Paramvir Bahl, and Hari Balakrishnan. Glimpse: Continuous, real-time object recognition on mobile devices. In *SenSys*, 2015.
- [32] Xukan Ran, Haolianz Chen, Xiaodan Zhu, Zhenming Liu, and Jiasi Chen. Deepdecision: A mobile deep learning framework for edge video analytics. In *INFOCOM*, 2018.
- [33] Anurag Ghosh, Srinivasan Iyengar, Stephen Lee, Anuj Rathore, and Venkata N Padmanabhan. React: Streaming video analytics on the edge with asynchronous cloud support. In *IoTDI*, 2023.
- [34] Philipp Bergmann, Tim Meinhardt, and Laura Leal-Taixe. Tracking without bells and whistles. In *ICCV*, 2019.
- [35] Daniel Bolya, Sean Foley, James Hays, and Judy Hoffman. Tide: A general toolbox for identifying object detection errors. In *ECCV*, 2020.
- [36] Joseph Redmon, Santosh Divvala, Ross Girshick, and Ali Farhadi. You only look once: Unified, real-time object detection. In *CVPR*, 2016.
- [37] Tsung-Yi Lin, Michael Maire, Serge Belongie, James Hays, Pietro Perona, Deva Ramanan, Piotr Dollár, and C Lawrence Zitnick. Microsoft coco: Common objects in context. In *ECCV*, 2014.
- [38] Arash Tavakoli, Fabio Pardo, and Petar Kormushev. Action branching architectures for deep reinforcement learning. In *AAAI*, 2018.
- [39] Ming-Fang Chang, John Lambert, Patsorn Sangkloy, Jagjeet Singh, Slawomir Bak, Andrew Hartnett, De Wang, Peter Carr, Simon Lucey, Deva Ramanan, and James Hays. Argoverse: 3d tracking and forecasting with rich maps. In *CVPR*, 2019.
- [40] Olga Russakovsky, Jia Deng, Hao Su, Jonathan Krause, Sanjeev Satheesh, Sean Ma, Zhiheng Huang, Andrej Karpathy, Aditya Khosla, Michael Bernstein, et al. Imagenet large scale visual recognition challenge. *IJCV*, 2015.
- [41] A visual walkthrough of streaming perception solutions. <https://mtli.github.io/streaming-streaming-visuals.html>, 2021.
- [42] Kai Chen, Jiaqi Wang, Jiangmiao Pang, Yuhang Cao, Yu Xiong, Xiaoxiao Li, Shuyang Sun, Wansen Feng, Ziwei Liu, Jiarui Xu, Zheng Zhang, Dazhi Cheng, Chenchen Zhu, Tianheng Cheng, Qijie Zhao, Buyu Li, Xin Lu, Rui Zhu, Yue Wu, Jifeng Dai, Jingdong Wang, Jianping Shi, Wanli Ouyang, Chen Change Loy, and Dahua Lin. MMDetection: Open mmlab detection toolbox and benchmark. *arXiv preprint arXiv:1906.07155*, 2019.
- [43] Kai Kang, Hongsheng Li, Junjie Yan, Xingyu Zeng, Bin Yang, Tong Xiao, Cong Zhang, Zhe Wang, Ruohui Wang, Xiaogang Wang, et al. T-cnn: Tubelets with convolutional neural networks for object detection from videos. *Transactions on Circuits and Systems for Video Technology*, 2017.

- [44] Akshay Uttama Nambi, Adtiya Virmani, and Venkata N Padmanabhan. Farsight: A smartphone-based vehicle ranging system. *IMWUT*, 2018.
- [45] Akshay Uttama Nambi, Ishit Mehta, Anurag Ghosh, Vijay Lingam, and Venkata N Padmanabhan. Alt: towards automating driver license testing using smartphones. In *Proc. SenSys*, 2019.
- [46] Songtao He, Favyen Bastani, Arjun Balasingam, Karthik Gopalakrishna, Ziwen Jiang, Mohammad Alizadeh, Hari Balakrishnan, Michael Cafarella, Tim Kraska, and Sam Madden. Beecluster: drone orchestration via predictive optimization. In *MobiSys*, 2020.
- [47] Arjun Balasingam, Karthik Gopalakrishnan, Radhika Mittal, Mohammad Alizadeh, Hamsa Balakrishnan, and Hari Balakrishnan. Toward a marketplace for aerial computing. In *Proceedings of the 7th Workshop on Micro Aerial Vehicle Networks, Systems, and Applications*, 2021.
- [48] Srinivasan Iyengar, Ravi Raj Saxena, Joydeep Pal, Bhawana Chhaglani, Anurag Ghosh, Venkata N Padmanabhan, and Prabhakar T Venkata. Holistic energy awareness for intelligent drones. In *BuildSys*, 2021.

Table 7: **Improvements on a predefined system. (ImageNet-VID)** All the execution policies operate on top of a perception system employing the same components: Faster R-CNN and Kalman Filter. We can observe similar trends to Argoverse-HD (Table 1).

Approach	sAP	sAP <sub>50</sub>	sAP <sub>75</sub>
1. Streamer ( $s = 600$ ) [6] (Static Policy)	34.4	59.8	35.4
2. Streamer + AdaScale [2] + Our Scheduler (Dynamic-Traditional Policy)	32.2	55.5	33.6
3. <b>Chanakya</b> ( $s = s_3, np = np_1, R = R_1$ )	<b>37.5</b>	<b>62.0</b>	<b>40.0</b>
4. <b>Chanakya</b> ( $s = s_3, np = np_1, R = R_2, \pi_{fixed} = (s = 480, np = 300)$ )	37.2	<b>62.0</b>	39.5

## A Implementation and Experimental Details

**Datasets.** We perform our experiments on the Argoverse-HD dataset [39, 6], which contains urban outdoor driving scenes from two US cities and ImageNet-VID dataset [40], which is a diverse dataset with 30 object categories.

**Performance Measure (mAP vs sAP):** Mean Average Precision or **mAP** is used to evaluate offline detection, where any detection for a frame is considered irrespective of its latency. Satisfying the formal definition above, Streaming AP or **sAP** [6] evaluates online or real-time detection, by matching the most recent detection that was provided on or before the current frame observed in a video stream. We evaluate real-time performance using the **sAP** measure, i.e., AP in the real-time setting, as it simultaneously evaluates both latency and average precision of the detections. Similar measures can be defined for other tasks like segmentation [6]. A visual walkthrough of sAP metric can be viewed in [41].

**Implementation Details.** We use the mmdetection [42] library to train and finetune our models. Further, while employing multiscale training on scales between [720, 320], we follow the *lx schedule* of mmdetection and default parameters to maintain consistency. We finetune our models from a base model trained on COCO [37], for ImageNet-VID we use the protocol described in [2, 43] and for Argoverse-HD we consider every 5<sup>th</sup> frame from the training sequences. Our controller is trained on the training set of these datasets, keeping model components frozen.

Evaluation is performed on the validation sets of ImageNet-VID and Argoverse-HD, as ground truth annotations for test set are not publically available. Unless stated otherwise, all our experiments are performed on Microsoft Azure’s ND-series machines with P40 GPUs. For training, we used machines with 4 GPUs and we evaluated on a machine with one P40 GPU.

**Controller training details.** Our controller is a 4 layer MLP with the hidden layer size of 256, input size being equal to the size of our context vector (i.e., 22 for Argoverse-HD and 44 for ImageNet-VID) and output size being the sum of each action dimension, i.e.  $\sum_i |D_i|$ . For epsilon-greedy exploration-exploitation, we set initial  $\epsilon$  as 1, decay rate as 0.999 and minimum- $\epsilon$  as 0.15 and train for 10 epochs. We train our models using both reward functions defined in Equations 1 and 2, which we refer to as  $R_1$  and  $R_2$ , respectively.

**Tradeoffs considered.** In our experiments, we defined the following decision dimensions: (1) **Scale (s):**  $s_1 = \{720, 640, 560, 480, 360\}$  and  $s_2 = \{750, 675, 600, 525, 450\}$ ;  $s_3 = \{600, 480, 420, 360, 300, 240\}$  (for fair comparison with AdaScale [2] on ImageNet-VID) (2) **Number of Proposals (np):**  $np = \{100, 300, 500, 1000\}$  (3) **Tracker scale (ts):**  $ts = \{720, 640, 560, 480, 360\}$  (4) **Tracker stride (k):**  $k = \{3, 5, 10, 15, 30\}$  and (5) **Model choice (m):**  $m = \{yolov3, fcos, frcnn\}$ .

While adapting to newer hardware, we considered additional decisions apart from Scale ( $s$ ) as  $s_4 = \{800, 880, 960, 1040, 1120, 1200\}$  and Number of Proposals ( $np$ ) as  $np_1$ . They are (1) **Models (m)** { $m = \{resnet\_frcnn, swin\_frcnn, resnet\_cascade\_rcnn, swin\_cascade\_rcnn\}$ } (2) **Inference Precision (p):**  $p = \{FP32, FP16\}$ .

**Results on ImageNet-VID** Improvements for a pre-defined system generalize to ImageNet-VID as we can observe in Table 7. From Figure 9, observe that the decisions for ImageNet-VID are different.

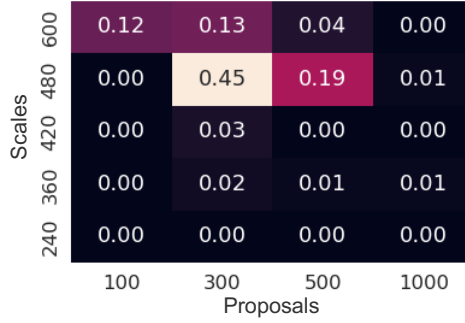


Figure 9: **Dynamic Configurations executed on P40 GPU. (ImageNet-VID)** For the predefined system, Chanakya changes the configuration depending on the intrinsics and achieves better performance. Notice that the runtime decisions are distinct from decisions taken in Argoverse-HD.

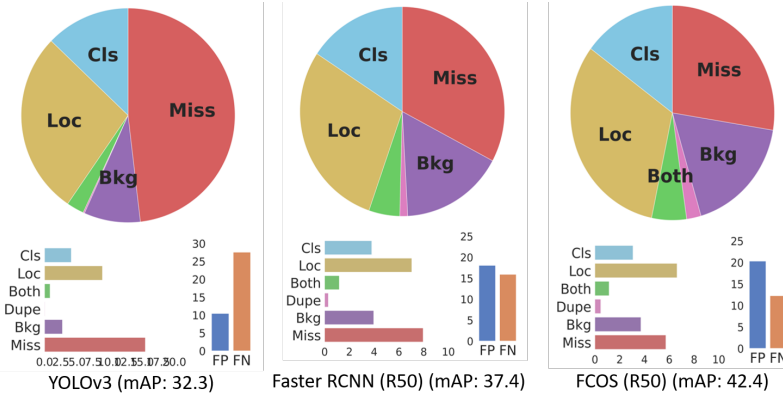


Figure 10: **Breakdown of Detection Errors on COCO using TIDE [35].** We can observe a much higher miss rate in YOLO compared to FCOS and Faster R-CNN.

## B Additional Details on Factors Influencing Runtime Decisions

Different models exhibit different error characteristics, Figure 10 and Figure 11 show the error breakdown for COCO [37] and ImageNet-VID [40]. The error breakdowns vary across the datasets among these models, and some models are more suited for specific scenarios.

## C Additional Details on Runtime Context

Table 8: **Switchability Classifier.** Switchability category acts as context for our controller to make a runtime decision. As we can observe, Classification performance on Argoverse-HD is far better than random selection, provided context is informative.

	Precision	Recall	F1-Score
Low	0.81	0.87	0.84
Medium	0.54	0.56	0.55
High	0.71	0.45	0.55
Accuracy			0.73

**Switchability Classifier.** To obtain this context, during training, we execute all the supported models  $F$  on image  $I$  to obtain detections  $\{x_{f_1}, x_{f_2} \dots x_{f_k}\}$ , where  $x_{f_i}$  is the output obtained from model  $f_i$ . We then compute the standard deviation of the mean IOU across all the models in  $F$  on  $I$  and

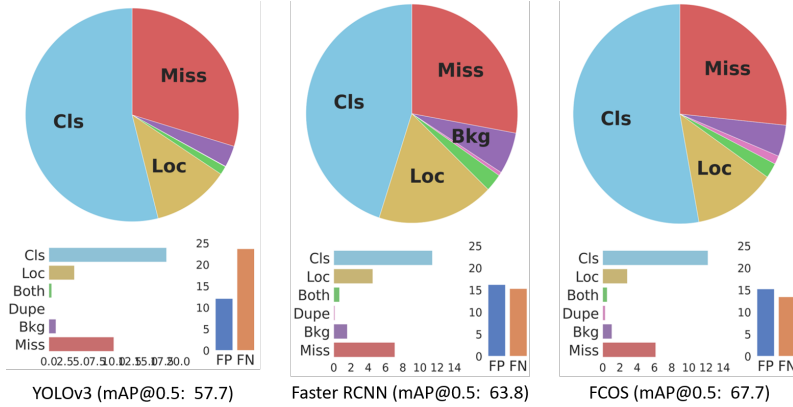


Figure 11: **Breakdown of Detection Errors on ImageNet-VID using TIDE [35]**. We can observe that classification errors dominate in this dataset, when compared to error breakdowns on COCO.

Table 9: **Overhead of Context**. While the context is obtained only when the controller is called to make a new runtime decision, there is an associated computational overhead. The overhead includes the runtime for the controller.

Scale	No Context	AdaScale	AdaScale + Scene Agg.	AdaScale + Scene Agg. + Switch.
900	104.1 ms	19ms	19.6ms	39.2ms
600	55.7ms	9.5ms	9.7ms	18.5ms
300	1.3ms	32.2ms	3.5ms	7.3ms

assign the switchability category to either, *low*, *medium*, or *high*. The *low* switchability category indicates that all the models (both expensive and inexpensive models) have similar performance and hence model switching is not particularly useful. Whereas, a *high* switchability category indicates switching will result in better accuracy. Finally, we train the classifier in a supervised manner, with input features from the backbone.

**Adaptive Scale Regressor.** We followed the method detailed in [2]. The regression target for an image is derived by comparing foreground box predictions at different scales (E.g., in our case  $s=\{720,600,480,360,240\}$ ). Common foreground objects have the minimum loss at the selected scale. We train a regressor in a supervised manner using these scale labels.

**Contention Sensor.** The contention generator is a CUDA kernel that performs arithmetic on arrays, following [4]. The contention levels are discrete in nature measured using `nvidia-smi` and `tegrastats` device as appropriate. Change in contention levels influences the latency of the detector as GPU cores are used by the generator.

**Overhead of Context.** Table 9 shows that the overhead of context for a single frame (presented numbers are averaged over 1000 distinct frames) at different scales is around 25-35%. The majority of the overhead is from the AdaScale regressor and switchability classifier. However, it should be noted that metrics are computed only when the controller is executed (i.e., once every 30 detection calls), hence, amortized overhead per frame is merely around 1% during runtime.

## D Additional Details on Learning the Controller

To learn  $Q_\theta$ , we employ a loss function that takes into account all the decision dimensions. The loss  $\mathcal{L}$  is calculated by sampling batch of  $\{\text{context}, \text{action and reward}\}$  tuples, i.e.,  $(z, a, r)$  from the controller’s replay buffer  $B$ ,

$$\mathcal{L} = \mathbb{E}_{(z, a, r) \sim B} \left[ \frac{1}{|\mathcal{D}|} \sum_{a_i \in a} [r - Q_\theta(z, a_i)]^2 \right]$$

---

**Algorithm 1:** Modified Shrinking Tail Scheduler

---

- 1: Given finishing time  $s$  and algorithm runtimes for different configurations  $\rho$  in the unit of frames (assuming  $\rho[i] > 1 \forall i$ ) and current algorithm configuration  $a$ , this policy returns whether the algorithm should wait for the next frame.
  - 2: Define tail function  $\tau(t) = t - \lfloor t \rfloor$
  - 3: **return**  $[\tau(s + \rho[a]) < \tau(s)]$  (Iverson bracket)
- 

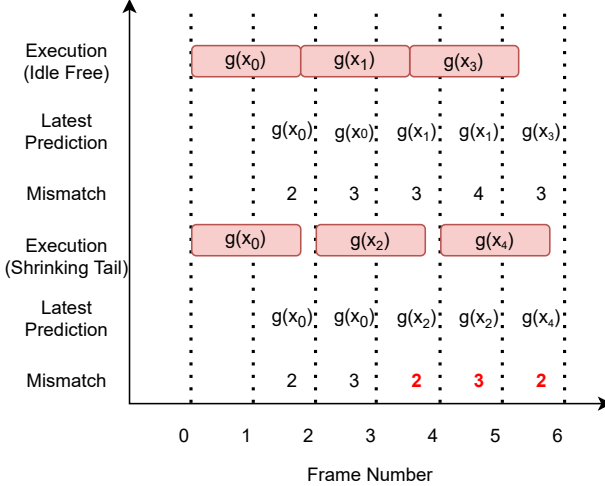


Figure 12: Temporal mismatch between the latest available prediction and the current frame in the stream employing Idle Free and Shrinking Tail scheduling of a function  $g$ . Lower mismatch (depicted in red) is better.

To perform exploration-exploitation during training, we employed UCB and  $\epsilon$ -greedy strategies. We empirically observed  $\epsilon$ -greedy converges faster and is our default strategy. While testing our learned policies, we act upon actions which provide the maximum expected reward given input context.

**UCB:** Action is chosen using the following equation,

$$a_\tau = \left\{ \underset{d \in D_i}{\operatorname{argmax}} \left[ Q_\theta(z_\tau, d) + c \sqrt{\frac{\ln(\tau)}{N_\tau(d)}} \right] \mid \forall D_i \in \mathbb{D} \right\} \quad (3)$$

where  $\tau$  denotes the number of trials.  $N_\tau(d)$  denotes the number of times that action  $d$  has been selected prior to step  $\tau$ , and the parameter  $c > 0$  determines the confidence level.

**$\epsilon$ -Greedy:** We set initial  $\epsilon$  as 1, and decay it by a factor till it reaches a minimum threshold. Action is chosen using via,

$$a_\tau = \begin{cases} \{d_i \sim U(D_i) \mid \forall D_i \in D\} & \text{with probability } \epsilon \\ \left\{ \underset{d \in D_i}{\operatorname{argmax}} Q_\theta(z_\tau, d) \mid \forall D_i \in D \right\} & \text{otherwise} \end{cases} \quad (4)$$

where  $U$  is uniform distribution.

## E Modified Shrinking Tail Scheduler

We discuss the difference between the scheduling algorithms that were mentioned in the main text. Figure 12 depicts temporal mismatch, the current frame number that has been received compared to the frame currently being processed. As expected, we would like mismatch values to be as close to zero as possible. Let's assume that the runtime of a detector is 60ms. We receive a new frame every 33ms. Say, we received frame 0 at  $t = 0$ ms, and started processing. Thus, we wait till 60ms for the result of Frame 0 by the time we have received Frame 1 for 27ms. At this point, we can make one of two choices, call the detector on Frame 1 (**idle-free scheduling**), or wait for 6ms to receive Frame 2

---

**Algorithm 2:** Obtaining Observations From Streaming Perception System

---

```

Initialize policy  $\pi$ 
Set change system configuration probability  $p$ 
 $\tau = 0$ 
for  $e = 0, 1, \dots, E - 1$  do
    Reset simulator;
    for every sequence do
        Initialize empty stream replay buffer  $S$ ;
         $i = 1$ ;
        while streaming do
            // System executes on streaming data
            ...
            value = Draw from Bernoulli( $p$ );
            if value == true then
                Observe  $x_i$  from the stream;
                 $z_\tau = \text{context}(x_i)$ ;
                 $a_\tau = \pi(z_\tau)$ ;
                Change system config. using  $a_\tau$ ;
                 $t_{a_\tau} = \text{time.now}()$ ;
                Store  $(z_\tau, a_\tau, t_{a_\tau})$  in stream replay buffer  $S$ ;
                 $\tau = \tau + 1$ ;
             $i = i + 1$ ;
         $\pi = \text{train\_controller}(\pi, S)$ ;
    
```

---



---

**Algorithm 3:** Training the Controller

---

```

Function train_controller( $\pi$ : Policy,  $S$ : Stream Replay Buffer):
    Unpack  $K$  length sequence
     $\{(z^1, a^1, t^1) \dots (z^K, a^K, t^K)\}$  from stream
    replay buffer  $S$ ;
    for  $n = 1, \dots, K$  do
         $r^n = R(t^n, t^{n+1})$ ;
        Store  $(z^n, a^n, r^n)$  in controller's replay buffer
         $B$ ;
     $\pi = \text{update}(\pi)$ ;


---


Update Policy


---


Function update( $\pi$ : Policy):
    // Optimize the  $Q$  function
    Sample  $N$  tuples
     $\{(z^1, a^1, r^1), \dots, (z^N, a^N, r^N)\}$  uniformly
    from buffer  $B$ ;
    for  $n = 1, \dots, N$  do
        // Set the targets
         $y^n = r^n$ 
    // Calculate the loss for the batch
     $\mathcal{L} = \frac{1}{N} \sum_{n=1}^N \frac{1}{|D|} \sum_{d \in a^n} [y^n - Q_\theta(z^n, d)]^2$ 
    Use optimizer to optimize  $\theta$  to minimize  $\mathcal{L}$ ;

```

---

and then make the blocking call (**shrinking tail scheduling**). Turns out, it's better to wait as that reduces the temporal mismatch [6].

As noted in Section 3.5, shrinking tail scheduler [6] assumes algorithm runtime is constant, which is not true in our case. However, the space of configurations is *discrete*, and runtime for *every* configuration can be assumed to be constant. Algorithm 1 incorporates that assumption.

## F Asynchronous Training

Asynchronous training strategy is conceptually simple, we train the controller only after one video stream (or sequence) is completely processed, as this sequence is streamed in real-time at 30 FPS. While the sequence is being processed in real time, we merely store the  $(z, a, t)$  tuples in a buffer  $S$  along with all the algorithm's predictions (to construct the reward  $r$ ). Then we add these tuples to controller's buffer  $B$  and sample from this buffer to update  $Q_\theta(z, a)$  via gradient descent. Algorithms 2 and 3 describe the strategy.

## G Deployment Efficiency.

Deployment efficiency is a critical factor when deploying to edge devices. Let us consider the scenario where our Chanakya has to learn tradeoffs for two dimensions,  $S = |D_s|$ ,  $P = |D_{np}|$ . We denote number of training epochs as  $n_{\text{epochs}}$ , number of training images as  $N_{\text{train}}$ , number of validation images as  $N_{\text{val}}$ , a scaling factor to accommodate for streaming scenarios  $\beta$  where  $\beta \geq 1$ , matrices  $M_{\text{prob}} \in \mathbb{R}^{S \times P}$  indicating the probability of an action chosen and  $M_{\text{lat}} \in \mathbb{R}^{S \times P}$  indicating latency. Time required for training Chanakya and other baselines can be formulated as:  $Chanakya_{\text{time}} = \frac{M_{\text{prob}} \cdot M_{\text{lat}}}{\beta} (n_{\text{epochs}} \cdot N_{\text{train}})$ . For static policy such as Streamer is  $Static_{\text{time}} = N_{\text{train}} \cdot \sum_{i \in D_s, j \in D_{np}} M_{\text{lat}}$  and for dynamic-offline policy such as AdaScale, it is  $Dynamic_{\text{time}} = \frac{N_{\text{train}} \cdot \sum_{i \in D_{\text{scale}}} M_{\text{lat}}}{\beta}$ .

We can now compute deployment efficiency of our approach against static and dynamic policies as:

$$\eta_1 = \frac{Static_{\text{time}}}{Chanakya_{\text{time}}} = \frac{\sum_{i \in D_s, j \in D_{np}} M_{\text{lat}}}{M_{\text{prob}} \cdot M_{\text{lat}} \cdot n_{\text{epochs}}}$$

$$\eta_2 = \frac{Dynamic_{\text{time}}}{Chanakya_{\text{time}}} = \frac{\sum_{i \in D_s} M_{\text{lat}}}{M_{\text{prob}} \cdot M_{\text{lat}} \cdot n_{\text{epochs}} \cdot \beta}$$

On Argoverse-HD containing approximately 55K images, Chanakya is 3.46x and 2.74x faster on the P40 server GPU and the Jetson Xavier NX respectively. The efficiency is slightly lower on the Jetson due to increased number of epochs during training. In case of dynamic-offline policy (AdaScale), since only one forward pass is required for all scales, AdaScale is twice as efficient as ours, but performs extremely poorly. Furthermore, deployment efficiency only increases as the configuration space combinatorially increases.

## H Application Scenarios

We briefly discuss two application scenarios, and observe how context and decisions change.

Consider a smartphone-based driver assistant [44, 45] employing vehicle detection and tracking. Process contention (from other mobile applications) and image content metrics form the context. We can assume the smartphone is deriving energy from the car and the expected response time is too low to perform remote execution on the cloud. Thus the decision dimensions are – detector resolution, tracker resolution and temporal stride, meta-parameters like number of proposals.

Consider another scenario, say, a drone survey platform [46, 47, 48] tasked with search and rescue operations. The drones have cloud support at the ground station along with onboard compute. The platform executes real-time person detection and tracking in the surveyed area. Here, the context is image content, energy use, device temperature, and dynamic network conditions, but not process contention. The decision dimension now includes remote execution on the cloud. The decision is thus affected by the context in new ways, for instance, if the decision is to execute to cloud machine, the detector choice and scale would now depend on network conditions [33].

For driver assistance application, developers need to decide the detector and tracker model, their scale, detector’s number of proposals, and tracker stride. Context provided to the decision function include the contention levels from other running processes apart from context derived from image content. Drone survey platform would have an additional binary decision to offload frames to the GPU on the edge-cloud ground station. Such additions can be accommodated in our decisions without any changes in training or scheduling algorithms. We can provide additional context (network conditions: latency and bandwidth, power etc) to Chanakya. Chanakya can be trained without changes for novel real-time perception scenarios (unlike [1, 32, 4, 30, 5]), highlighting its flexibility and adaptability.

Adopting Chanakya simplifies development cycle for real-time perception by letting developers focus on identifying and implementing context, and defining decisions which introduce computational tradeoffs. The developers provide models, the decision space, and a dataset for training Chanakya. Chanakya would automatically learn the decision function depending on the context and execute decisions with favorable tradeoffs. Chanakya imposes no restriction on task and can be applied to any task (detection, segmentation etc).